Advances in Cryogenic Structural Materials for Superconducting Magnets

J.W. Morris, Jr.
Lawrence Berkeley Laboratory, Materials and Molecular Research Division, Bldg. 62, Berkeley, California 94720, U.S.A.
E.N.C. Dalder
Lawrence Livermore National Laboratory P.O. Box 5511, L-643, Livermore, California 94550, U.S.A.

Abstract

This paper reviews research in the United States and Japan on structural materials for high-field superconducting magnets. Superconducting magnets are used for magnetic fusion energy devices and for accelerators that are used in particle-physics research. The cryogenic structural materials that we review are used for magnet cases and support structures. We expect increased materials requirements in the future.

Introduction

Materials needs for superconducting magnets are set by the requirements of the systems in which they are used. Superconducting magnets are used in several new technologies: magnetic fusion energy (MFE); accelerators for physics research; and nuclear magnetic resonance for medical diagnosis.

1. Fusion Energy Devices

Both MFE concepts for plasma confinement use high magnetic fields to confine the plasma and use superconducting magnets to create the magnetic field. For the toroidal or "tokamak" concept, the major test-facility in United States is the Tokamak Fusion Test Reactor (TFTR). The TFTR device uses fields that are about 10 T (tesla) at the magnet conductor ($\sim$5 T at the plasma center). The magnets are copper electromagnets. Superconducting magnets for tokamaks are being developed at the Large Coil Project (LCP) at Oak Ridge National Laboratory (ORNL). At ORNL six large 8-T magnets are being tested. These particular magnets were chosen to represent different design and materials concepts. Three were constructed in the United States, two in Europe, and one in Japan. Five use NbTi superconductor; the sixth, built by Westinghouse in the United States, uses Nb_3Sn superconductor.

A future tokamak called Tokamak Ignition and Burn Experimental Reactor, "TIBER" will require toroidal field (TF) coils with peak fields near 10 T at the conductor. Superconducting poloidal field coils will operate in the 7 to 15 T range. Another tokamak, Alcator DCT, being designed at the Massachusetts Institute of Technology (MIT),

will use 10-T toroidal magnets and 7-T poloidal magnets. The present MIT design uses Nb_3Sn toroidal coils and NbTi poloidal coils.

Tandem-mirror fusion confines the linear-cylindrical plasma at its ends using an arrangement of high-field magnets. The major tandem-mirror fusion facility in United States is the Mirror Fusion Test Facility (MFTF-B) located at Lawrence Livermore National Laboratory (LLNL). In MFTF-B, the plasma is contained in a central tube of solenoid magnets. The solenoid set is completed at each end by a combination of magnets, with a peak fields of 2 to 3 T in the solenoid, 12 to 13 T in the small axicells, 5 to 6 T in the transition coils, and 7 to 8 T in the yin-yang coil set. All magnets are superconducting. Two of the axicells have NbTi outer solenoids and Nb_3Sn inserts, with NbTi conductors in all other magnets. As of this writing (July 1985), all magnets are complete.

2. Materials Needs

Increasing device size and magnetic field increases loads on magnet structures. Present systems use existing alloys, future designs will require alloys that offer superior combinations of yield strength (σ_y) and fracture toughness (K_{IC}) at 4 K.

Precise materials requirements depend on which of two structural support schemes is used and on the detailed magnet designs. In the most common support scheme, superconductors are supported by external magnet cases as in MFTF and by several coils in LCP. In an alternative support design, the superconductors are placed inside high-strength tubes that provide internal support; consequently, the case is a low-strength aluminum alloy or stainless steel. The superconductor in this support design is a cable that is "force-cooled" by flowing He. This type of superconductor is used in the Westinghouse LCP Nb_3Sn coil and is also the current choice for the Alcator DCT and TIBER.

Conventional austenitic stainless steels are used in external magnet cases [1]. These alloys offer combinations of σ_y and K_{IC} at 4 K (Fig. 1) that meet MFTF requirements and can be welded with available techniques and filler metals [2]. Future MFE magnets will require superior materials. Figure 1 shows the projected design requirements developed by Japan Atomic Energy Research Institute (JAERI) for a future tokamak machine [3]. These requirements call for σ_y:K_{IC} combinations that are beyond the capabilities of existing stainless steels. Additional studies suggest that the JAERI design goals are more readily available.

Because of conductor manufacturing methods, force-cooled Nb_3Sn conductors present unusual materials requirements [4]. For these conductors, a thin sheet is wrapped around conductor-wires and is longitudinally seam-welded to make tubes before the wire is heat-treated to form Nb_3Sn. The sheet must have good σ_y and K_{IC} at 4 K after welding and heat exposure in the range 600 to 800°C for times to 250 hours. An Fe-base alloy, JBK-75 (a modified alloy A286), was used for the tubes in the Westinghouse LCP coil and was aged at 700°C for 30 hours to form Nb_3Sn. However, JBK-75 forms undesirable phases when aged at higher temperatures or for longer time periods. The alloy's coefficient of thermal contraction is too large, and when cooling to 4 K, the tube strains the Nb_3Sn. New materials are needed for Nb_3Sn force-cooled conductor tubes [5].

3. Materials for Magnet Cases

Materials for MFE magnet cases must be strong, tough, inexpensive, and resistant to fatigue in welded structures at 4 K. Material response to radiation is of interest and will be critical in future machines that operate at end-of-life neutron fluences beyond 10^{19} neutrons per cm^2 (E > 0.1 MeV). Three alloy classes that may meet these needs are the following: modified Fe-Ni-Cr austenitic steels, modified Fe-Mn-Cr austenitic steels, and modified Fe-Ni ferritic steels.

3.1. Fe-Ni-Cr Austenitic Steels

Strength-toughness characteristics of Fe-Ni-Cr stainless steels are shown in Fig. 1. These alloys have adequate σ_y and K_{IC} to meet current, but not future needs. Researchers at Nippon Steel have made large improvements in σ_y:K_{IC} tradeoffs by using a high-purity melting practice to minimize inclusion content [6]. Initial properties of such alloys are attractive. Whether these alloys, with their expected high costs, can be fusion-welded and still retain sufficient purity and properties in the weld-metal and heat-affected zone must be determined.

A second way to improve the 4-K σ_y:K_{IC} tradeoff is to add Mn to the Fe-Ni-Cr alloy. This technique increases nitrogen solubility and the resulting interstitial solid-solution hardening. A high-strength-alloy "Nitronic 40" (21Cr-6Ni-9Mn-0.2N) with a 4-K σ_y of 1380 MPa is an example. However, such alloys embrittle, with 4-K K_{IC} values of less than 100 MPa $(M)^{1/2}$. These alloys are not fusion-weldable for 4-K service because of high levels of brittle δ-ferrite and/or formation of intermetallics in the weld metal [7].

3.2. Fe-Mn-Cr Austenitic Steels

A second class of austenitic steel is based on the Fe-Mn-Cr system. Most alloy development has been done in Japan. These alloys have good 4-K σ_y:K_{IC} tradeoffs at low cost and are designed for 77- and 4-K applications.

The Fe-Mn system undergoes mechanical twinning and transformation to hexagonal ε-martensite phase [8]; these two phenomena are related. Twins, or Face-Centered Cubic (FCC) basal-plane faults, introduce an element of hexagonal phase. Hexagonal ε-martensite is found in quenched structures at Mn contents intermediate between the ε-martensite and stable γ regions, i.e., between 10 and 30 weight percent Mn (Fig. 2). Martensite also forms through strain-induced transformation of residual γ in alloys in this composition range (Fig. 3). The ε-phase increases strength, but decreases toughness [9]. There is a large minimum in cryogenic K_{IC} of Fe-Mn alloys at 25% Mn (Fig. 3) that is larger than is explained from strength increases alone.

Additions of Cr, C, or N_2 decrease the ease of ε-formation and improve the σ_y:K_{IC} tradeoff. Carbon and N_2 are effective interstitial strengtheners in Fe-Mn alloys (Fig. 4) [10]. Nitrogen is preferred; C forms precipitates during heat treatment or welding that degrade toughness [11]. Because Mn increases N solubility in austenite, the addition of N increases 4-K σ_y to high levels.

Chromium stabilizes austenite in high Mn alloys, and improves corrosion resistance if present in an amount above about 12%, making such Fe-Mn-Cr alloys stainless. Brittle intermetallics form at higher Cr contents, particularly in weldments and castings, so small amounts of Ni are added to stainless grades to stabilize γ.

An Fe-Mn based alloy with a stable austenitic microstructure deforms by microtwinning, causing high work-hardening rates and complex substructures. Hence, Fe-Mn alloys tolerate inclusions and have good toughness even when impure. The Fe-Mn based austenites respond well to cold work, adding appreciable amounts of σ_y with small losses in K_{IC}.

Two classes of Fe-Mn-Cr alloys exist that differ in Cr and Ni contents. The nonstainless grades include the 25Mn-5Cr alloy developed at Nippon Steel for use at 77 K [11] and the 32Mn-7Cr alloy developed by Japan Steel Works [12].

Exceptional cryogenic properties are achievable in stainless Fe-Mn-Cr alloys (Fig. 5) for a 18Mn-16Cr-5Ni-0.22N alloy [10]. This alloy has 4-K σ_y:K_{IC} tradeoffs that are superior to conventional austenitic-stainless steel tradeoffs. This alloy also retains its toughness advantage after rolling. Tested after rolling at 1200°C, this alloy met JAERI requirements for σ_y:K_{IC} tradeoffs.

Stainless Fe-Mn-Cr alloys have good fatigue resistance [13]. Figure 6 compares the 4-K fatigue crack-growth rate (FCGR) of the 18Mn-15Cr-5Ni-0.22N alloy with the FCGRs of the conventional stainless steels 304 and 304LN. The FCGR of the hot-rolled Fe-Mn-Cr alloy is well below that of 304LN, and less than that of the metastable austenitic alloy 304. Also, the Fe-Mn-Cr alloy has much higher σ_y.

Properties of stainless Fe-Mn-Cr-N steels were confirmed in work on a 22% Mn modification by Kobe Steel and JAERI [14]. The alloy is made in commercial heats that meet JAERI needs. Weldability of these alloys has not been determined. Favorable σ_y:K_{IC} behavior is due to residual mechanical work in the microstructure. Candidate welding methods must preserve or duplicate this microstructure to ensure comparable behavior.

3.3. Ferritic Cryogenic Steels

Austenitic steels are used for magnet cases because they have good cryogenic K_{IC} in the mill-annealed condition and low magnetic susceptibility. The latter requirement is no longer necessary, because the presence of saturated ferromagnetic materials does not degrade magnetic performance. The JBK-75 superalloy used for conductor tubes in the Westinghouse large coil is ferromagnetic at 4 K. Cryogenic brittleness of ferritic alloys remains a problem. Ferritic alloys now available have ductile-brittle transition temperatures (DBTT) above 4 K. Present ferritic alloys offer advantages for magnet cases. They are relatively cheap alloys that reach strength levels near 1380 MPa. Alloy design efforts are underway in the United States and Japan to develop ferritic steels for magnet cases. Alloys and thermal treatments are needed that suppress transition temperatures (T_B) to below 4 K. Iron-Ni ferritic steels based on Fe-(9-12)Ni are routinely used at temperatures of 77 K.

The DBTT problems in 9-12Ni steels can be understood by following their transformation from γ to a lath martensite whose basic element is a "packet" of parallel laths (Fig. 7). The laths follow $\{100\}$ cleavage planes and fracture as a unit under

stress. On cooling, the alloy's strength increases until the cleavage stress is exceeded in highly-stressed regions ahead of crack tips, with brittle fractures through successive cleavage of martensite packets along {100} planes [15].

To decrease T_B, the martensite packet size is refined in these steels. One way is to put in a controlled distribution of precipitated γ along martensite lath boundaries through an intercritical temper (Fig. 8) [16]. This γ breaks up martensite packet alignment, increases resistance to cleavage fracture, and decreases DBTT. Another way is to heat treat the alloy to reduce packet size by thermal-cycling treatments that either recrystallize the prior austenite grains, decreasing the maximum packet size, or directly destroy crystallographic alignment of adjacent laths to achieve a fine grain size [17]. Useful treatments alternate a thermal cycle into the γ stability field (α reversion treatment) with a thermal cycle in the upper part of the γ stability field (intercritical anneal). A four-step cycle of this type [8], the "2B" treatment, produced a very good combination of σ_y and K_{IC} near 4 K in an Fe-12Ni-0.25Ti alloy. Recent versions of these alloys are shown in Fig. 9 [18].

Cryogenic σ_y:K_{IC} tradeoffs for Fe-12Ni-0.25Ti, processed as above, are compared with σ_y:K_{IC} tradeoffs for austenitic stainless steels and with JAERI requirements (Fig. 10). Ferritic alloys are made with 4-K σ_y:K_{IC} tradeoffs above those of current stainless steels, but do not yet have K_{IC} to meet the JAERI needs. Fracture modes in the best alloys are not completely ductile. Improvements in processing ferritic steels should yield substantial increases in K_{IC}.

Ferritic alloys have excellent weldability for 4-K service. The best Fe-Ni alloy heat treatment is a rapid thermal cycle into the γ field. A rapid reversion cycle decomposes lath alignment within martensite packets, creating fine grain size [19]. Rapid thermal cycles occur if alloys are welded with processes where each weld pass is repeatedly heated by subsequent passes, such as the gas-tungsten-arc (GTA) welding techniques used by Kobe Steel and Nippon Kokan to weld 9Ni steel for use at 77 K and above [20]. Modifications of this process yield weldments that have high K_{IC} at 4 K [21]. The usefulness of multipass welding is illustrated by a K_{IC} result taken from a weld-plate sample made from Kobe Steel Corporation's 11Ni weld metal from a multipass GTA welding process [18]. The plate was all weld metal and had a 4-K K_{IC} above 121 MPa $(M)^{1/2}$. Flaws in the weld appeared as brittle regions in the fracture surface. Improved welding techniques will produce higher K_{IC} values.

3.4. Structural Alloys for Force-Cooled Conductors

The manufacturing method for force-cooled conductor tubes is described in Section 2. For NbTi superconductors, tubes are made of any suitable conventional stainless steel. For Nb_3Sn conductors, reacted after assembly, the sheath must be an alloy that combines tolerance for long-time, high-temperature reaction treatments with good σ_y:K_{IC} tradeoffs at 4 K. Conventional austenite stainless steels are unsuitable for Nb_3Sn conductor conduits because intermetallic phases such as $M_{23}(C,N)_6$ and σ form in weld and base metals after prolonged heating at high temperatures.

The tube alloy used in the Westinghouse large coil was JBK-75, with a nominal composition of Fe-29Ni-15Cr-2Ti-1.25Mo-0.25Al-0.25V-0.016C. During heat treatment, this

alloy hardens through precipitation by forming the ordered intermetallic phase, γ', $Ni_3(Ti,Al,Mo)$. The JBK-75's σ_y depends only slightly on temperature, but exceeds 1000 MPa at 4 K after 10 to 15% cold work and a 700°C/30-hour heat treatment. This alloy's ductility and K_{IC} remain high after autogenous GTA welding and post-weld processing.

However, JBK-75 is not suitable for tubes in the Alcator DCT and TIBER, which will operate at higher fields (10 to 15 T). This higher field places stringent demands on Nb_3Sn conductor performance. To improve critical current, double-aging treatments (such as 700°C/2 days plus 730°C/2 days) must be used. Higher temperatures and longer time periods cause γ' to transform to equilibrium η phase along grain boundaries with serious losses of K_{IC}. The JBK-75 has a greater thermal contraction than Nb_3Sn, thereby compressing the superconductor and causing a big decrease in its critical current at fields above 8 T. Alloys under study for these applications are low-expansion Fe-Ni-Co superalloys [22] such as Incoloy 903(Fe-39Ni-14Co-3Nb-1.4Ti-0.9Al) with thermal contractions close to that of Nb_3Sn from 300 to 4 K. Incoloy 903 hardens by precipitation of ordered intermetallic γ', $Ni_3(Nb,Ti,Al)$. The addition of Nb improves aging response and slows overaging kinetics.

Changes in tube alloys for advanced tokamak magnets is a trend in alloys for force-cooled Nb_3Sn conductor tubes. Future tube alloys must have the necessary cryogenic structural properties and also must match the functional properties of superconductors. The alloys will be tailored to the design and may differ from one magnet to another.

4. Conclusions

This review covers some of the variety of engineering initiatives and materials research activities that bear on the development of high-field superconducting-magnet technology. The work that is described here shows that cryogenic materials research is an active and exciting area that addresses important technological needs in real devices and is systematically satisfying those needs through sophisticated materials research.

Acknowledgments

The authors appreciate the assistance of D. Dietderich, W. Hassenzahl, H. J. Kim, B. Fultz, and J. Glazer all of the Lawrence Berkeley Laboratory. This work was supported by the Director, Office of Energy Research, Office of Development and Technology, Magnetic Systems Division of the U.S. Department of Energy under contract DE-AC03-76SF00098 and also at Lawrence Livermore National Laboratory under Department of Energy contract W-7405-ENG-48.

REFERENCES

/ 1 / C. D. Henning and E. N. C. Dalder, in the Proc. of Structural Mechanics in Reactor Technology, West Berlin, Germany, August 1979.

/ 2 / C. D. Henning et al., in the Proc. of the Eighth Symposium on Engineering Problems of Fusion Research, San Francisco, November 1979, p. 84.

/ 3 / H. Nakajima et al., Adv. Cryog. Eng., 30, 219 (1983).

/ 4 / R. E. Gold et al., Adv. Cryog. Eng., 28, 759-771 (1981).

/ 5 / M. O. Hoenig et al., in Proc. of Int. Mag. Tech., Grenoble, 1983.

/ 6 / H. Masumoto et al., Adv. Cryog. Eng., 30, 169 (1984).

/ 7 / M. J. Strum, M. S. Thesis, Dept. Materials Science, Univ. of California, Berkeley, LBL Rept. 14750 (1982).

/ 8 / J. W. Morris, Jr. et al., Advances in Cryogenics Engineering, 24, 91 (1978).

/ 9 / Y. Tomota and J. W. Morris, Jr., in Proc. of Int. Cryogenic Materials Conf., Kobe, 1982, A. F. Clark and K. Tachikawa, Eds., (1982) p. 124.

/ 10 / R. Ogawa and J. W. Morris, Jr., in the Proc. of Int. Cryogenic Materials Conf., Kobe, 1982, A. F. Clark and K. Tachikawa, Eds. (Butterworths, London, 1982) p. 124.

/ 11 / H. Yoshimura et al., Adv. Cryog. Eng., 28, 115 (1982).

/ 12 / R. Miura et al., Adv. Cryog. Eng., 30, 245 (1983).

/ 13 / R. Ogawa and J. W. Morris, Jr., in the Proc. of TMS-AIME Symposium on Fatigue at Low Temperatures, Louisville, KY., May, 1983.

/ 14 / Y. Kasamatsu et al., Adv. Cryog. Eng., 30, 145.

/ 15 / J. I. Kim et al., Met. Trans. 14A, 93 (1983).

/ 16 / H. J. Kim et al., Met. Trans., (in press).

/ 17 / S. Jin, J. W. Morris, Jr., and V. F. Zackay, Met. Trans., 6A, 129 (1975).

/ 18 / H. J. Kim, Lawrence Berkeley Laboratory, Berkeley, CA, unpublished research, (1984).

/ 19 / M. Niikura and J. W. Morris, Jr., Met. Trans., 11A, 1531 (1980).

/ 20 / K. K. Nippon Kokan, Presented at 1980 AWS 61st Annual Meeting, Session 22.

/ 21 / H. J. Kim, H. K. Shin, and J. W. Morris, Jr., in the Proc. of the International Cryogenic Materials Conference, Kobe, Japan, A. F. Clark and K. Tachikawa, Eds. (Butterworths, London, 1982) p. 129.

/ 22 / M. M. Steeves, M. O. Hoenig, and C. J. Cyders, Adv. Cryog. Eng., (in press).

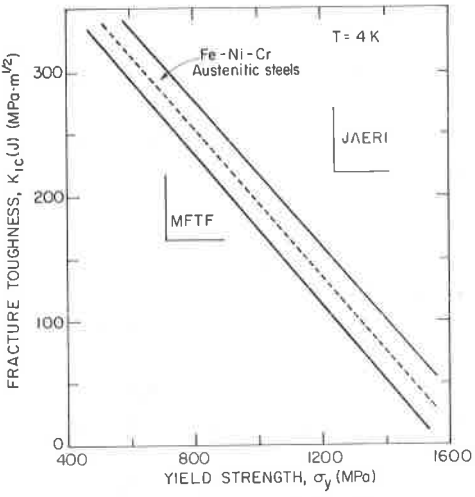

Fig. 1. Strength-toughness trend for Fe-Ni-Cr alloys at 4 K.

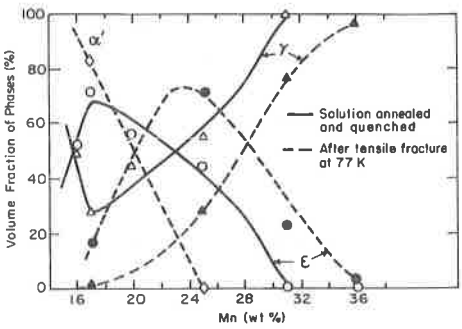

Fig. 2. Phases present in Fe-Mn binary alloys as a function of composition. Solid lines show the phase distribution in the as-quenched state. Dashed lines show the distribution after straining at 77 K.

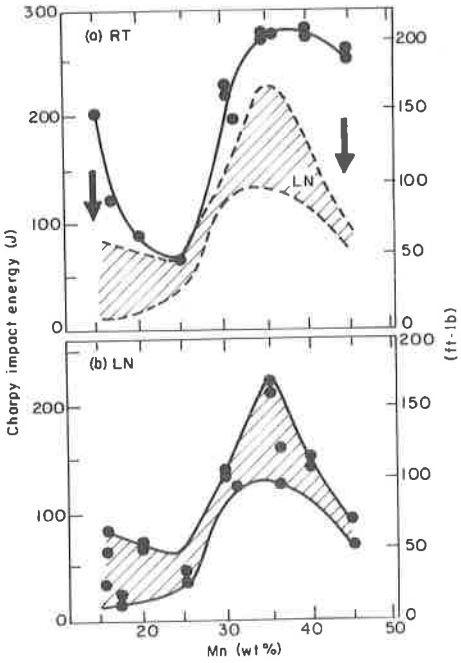

Fig. 3. Toughness vs Mn content for Fe-Mn binary alloys at room temperature and at 77 K.

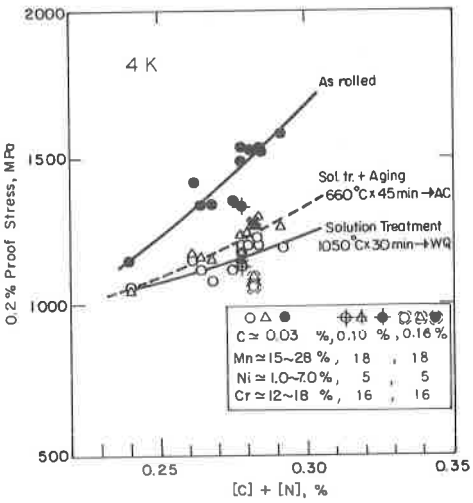

Fig. 4. Increase in yield strength with carbon and nitrogen addition in Fe-Mn binary alloys.

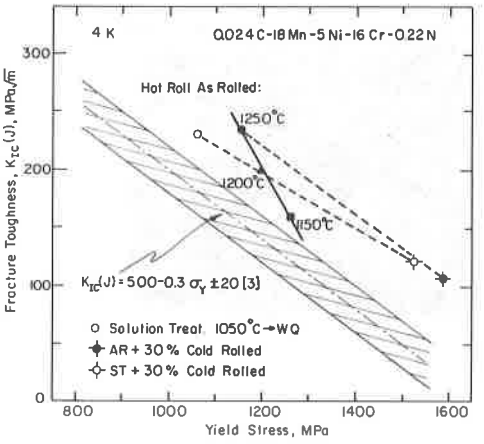

Fig. 5. Strength-toughness combinations of a Fe-Mn-Cr-Ni alloy at 4 K as functions of processing.

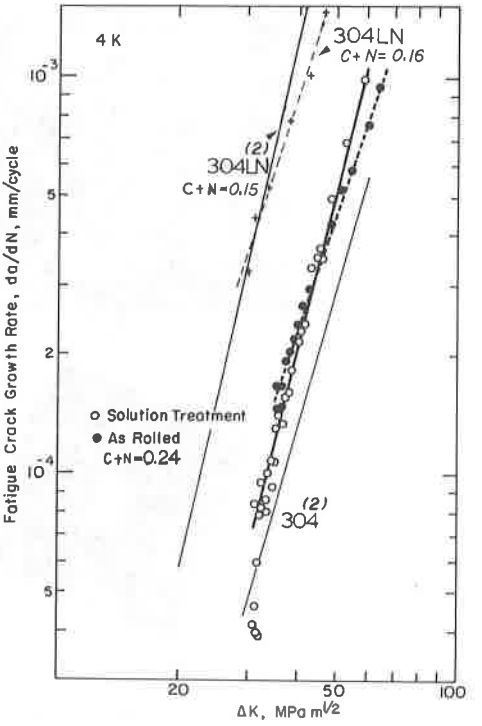

Fig. 6. Fatigue-crack-growth rate of an Fe-Mn base alloy at 4 K compared with that of the conventional stainless steels 304LN and 304.

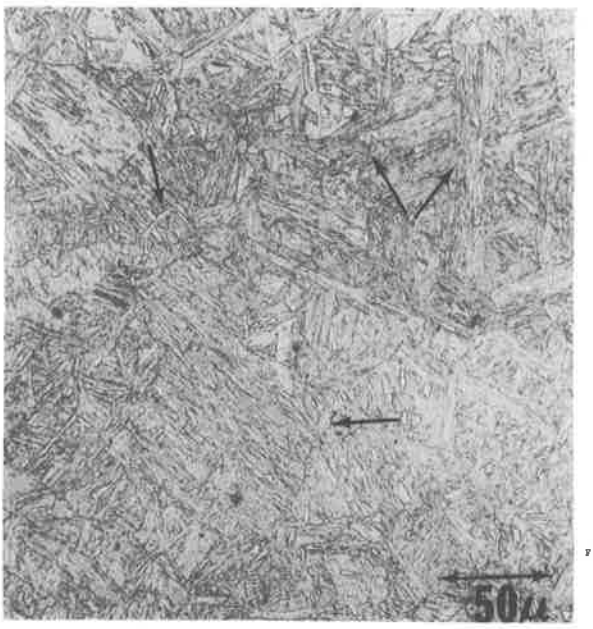

Fig. 7. Optical micrograph of an Fe-Ni cryogenic steel showing grouping of laths into packets.

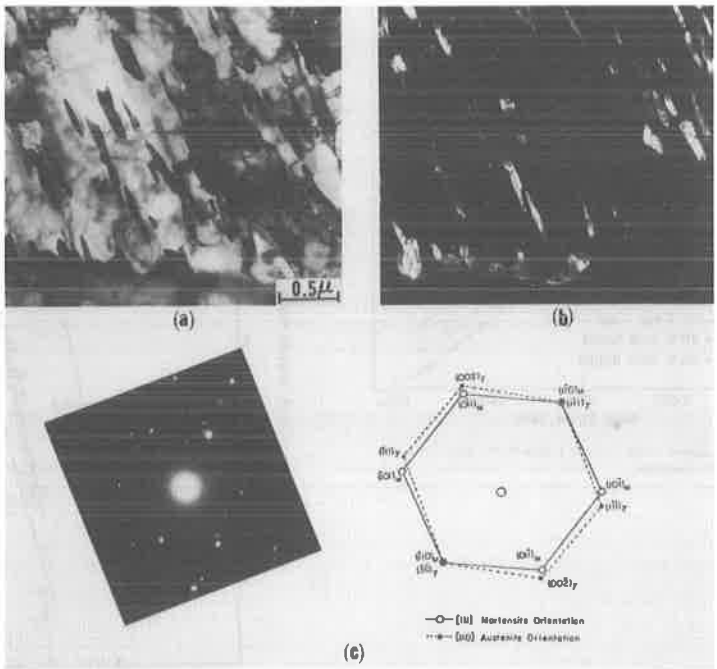

Fig. 8. Transmission electron micrograph of intercritically-tempered Fe-Ni cryogenic steel showing precipitated austenite along lath boundaries. Figure (b) is a dark field micrograph taken from an austenite diffraction spot.

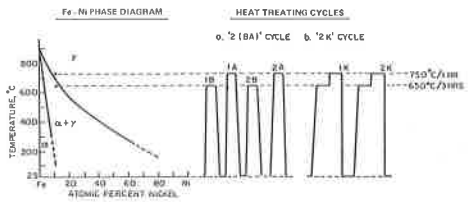

Fig. 9. Thermal-cycling treatments used in processing Fe-12Ni-0.25Ti for toughness at 4 K.

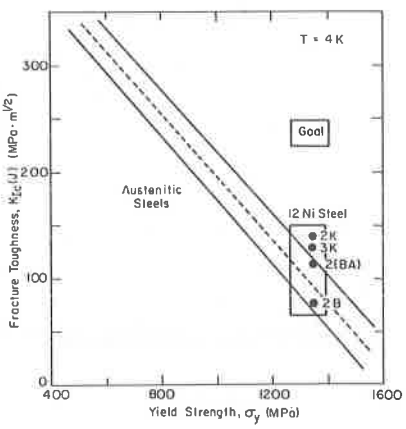

Fig. 10. The 4-K strength-toughness combinations of Fe-12Ni-0.25Ti processed through thermal cycle treatments shown in Fig. 9.